3D near-infrared imaging based on a single-photon avalanche diode array sensor

Juan Mata Pavia[a,b], Edoardo Charbon[b,c], Martin Wolf[a]

[a]University Hospital Zürich(USZ), Biomedical Optics Research Laboratory(BORL), Division of Neonatology, 8091 Zürich, Switzerland
[b]Ecole Polytechnique Fédérale de Lausanne (EPFL), Quantum Architecture Group(AQUA), 1015 Lausanne, Switzerland
[c]TU Delft, 2628CD Delft, Netherlands

ABSTRACT

An imager for optical tomography was designed based on a detector with 128x128 single-photon pixels that included a bank of 32 time-to-digital converters. Due to the high spatial resolution and the possibility of performing time resolved measurements, a new contact-less setup has been conceived in which scanning of the object is not necessary. This enables one to perform high-resolution optical tomography with much higher acquisition rate, which is fundamental in clinical applications. The setup has a resolution of 97ps and operates with a laser source with an average power of 3mW. This new imaging system generated a high amount of data that could not be processed by established methods, therefore new concepts and algorithms were developed to take full advantage of it. Images were generated using a new reconstruction algorithm that combined general inverse problem methods with Fourier transforms in order to reduce the complexity of the problem. Simulations show that the potential resolution of the new setup is in the order of millimeters. Experiments have been performed to confirm this potential. Images derived from the measurements demonstrate that we have already reached a resolution of 5mm.

Keywords: Near-infrared spectroscopy (NIRS), Near-infrared imaging NIRI, Time-resolved imaging, Image reconstruction techniques, Diffuse optical tomography, Inverse problems, CMOS, SPAD, Time-of-flight camera, Single-photon detector.

1. INTRODUCTION

Optical tomography has been traditionally characterized by low resolution and poor image quality. Recently, researchers have demonstrated that it is possible to improve the image quality by using large data sets coming from CCD cameras.[1,2] The proposed systems scan the surface of the object under study using continuous-wave (CW) lasers or illuminate them with spatially modulated light.[3] Although there have been attempts of using time-resolved methods in combination with large data sets by using intensified CCD cameras, these systems have major performance restrictions, thus limiting their suitability.[4] Time-resolved techniques enable better depth resolution, thus improving the quality of the reconstructions and they are better suited to resolve absorption and scattering.[5]

In this paper, the aim is to show how recently developed single-photon avalanche diode (SPAD) array imagers[6] can open new frontiers in time-resolved optical tomography. These new sensors combine high spatial resolution images with picosecond time-resolved measurements, bringing together the advantages of using discrete components for time-resolved measurements and CCD cameras. The presented setup does not require raster scanning the surface of the tissue or any other change in the properties of the illumination source. A new theoretical framework has been developed to model the propagation of cylindrical waves in highly scattering media and reconstruct heterogeneities embedded in it.

Send correspondence to J. Mata Pavia, UniversitätsSpital Zürich, Klinik für Neonatologie, Frauenklinikstrasse 10, 8091 Zürich, Switzerland, E-mail: juan.matapavia@epfl.ch, Telephone: +41 (0)44 556 3032

2. SETUP

Although illumination with plane waves has shown to reduce the complexity of reconstruction algorithms,[1] it is not possible to use this approach with this sensor due to the fast temporal response of backscattered light with plane waves. In terms of temporal response, image contrast and resolution, this approach would be similar to zero distance source-detector approaches used in near-infrared spectroscopy.[7] Monte Carlo simulations[8] show that in this kind of experiments the optical signal has a dynamic range of more than 50dB per nanosecond.For this reason, a new illumination system has been conceived that trades off image reconstruction complexity with sensor speed. The solution adopted was to illuminate the object under study with lines outside the field of view of the camera. Thus,the light captured by the sensor undergoes several scattering events before it is detected, making its temporal point-spread function (TPSF) much smoother. The SPAD sensor used in this work is implemented

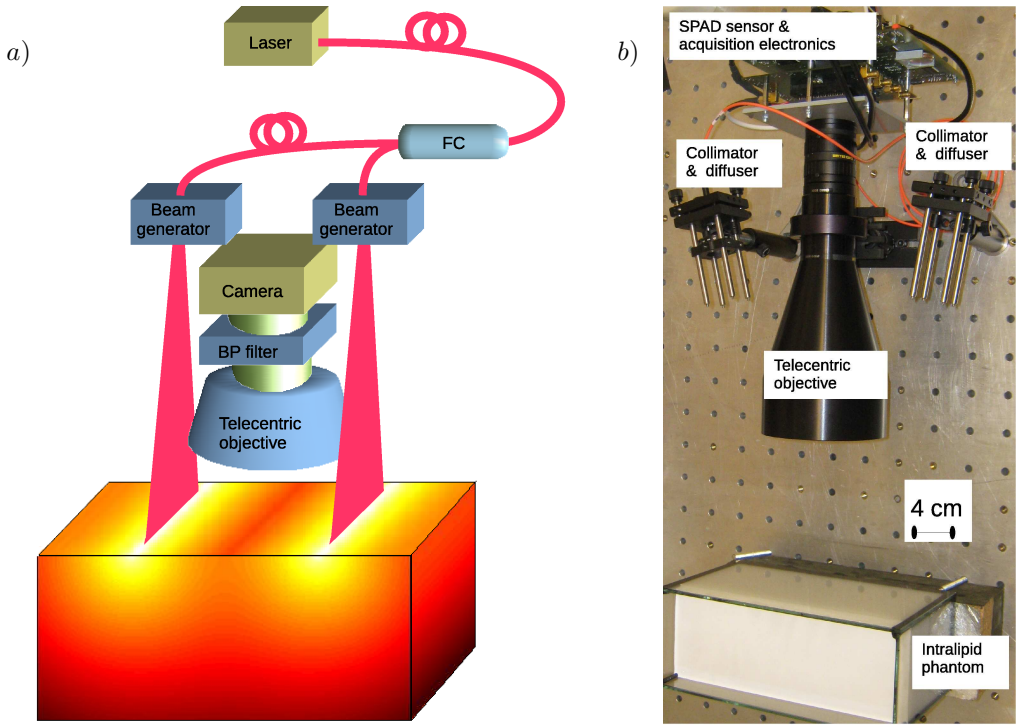

Figure 1. a) Diagram of the new optical setup for NIRI. A picosecond laser is used to generate lines of light on the surface of the object under study. b) Setup implementation.

in a standard CMOS 0.35μm process. It has 128x128 pixels connected to 32 time-to-digital converters (TDCs) with a resolution of 97ps.[6] This detector works in time-correlated single-photon counting (TCSPC) mode and provides time-resolved measurements for each of its pixels, independently. A Becker&Hickl BHLP-700 laser with an average power of 3mW is used as light source. Two parallel lines on the tissue by means of a fiber coupler and two diffusers and collimators. A telecentric objective with high numerical aperture is used to focus the backscattered light from the tissue into the SPAD imager. Figure 1 shows the new optical setup.

For the experiments, we use an intralipid phantom as target. It is composed of distilled water, intralipid emulsion and Indian ink. Small heterogeneities made of silicon, TiO_2 and carbon powder are introduced in the phantom in order to be reconstructed. Those heterogeneities have the same reduced scattered coefficient μ_s' as the intralipid phantom but a higher absorption coefficient μ_a. The reconstruction algorithm is capable of reconstructing absorption and scattering changes simultaneously, however experiments have been performed only with absorption heterogeneities as scattering produce smaller changes in the measured field, and there is always some crosstalk between the two parameters during the reconstruction process.

3. THEORY

We use the diffusion approximation for the photon density $u(\vec{r},\omega_t)$ in a diffusive media produced by a harmonically time modulated source[9] $S(\vec{r},\omega_t)$, resulting in Eq. (1), where μ_s' and μ_a are assumed to be constant and ν is the speed of light in the medium. If the source term $q(\vec{r},\omega_t)$ is x independent, then the solution of (1) in a homogeneous infinite medium is Eq. (4), where $H_0^{(1)}$ is a Hankel function of the first kind, $\vec{r}_{yz}=(y,z)$, and $\vec{r}_{yz}^{\,0}$ is the position of the source.

$$\nabla^2 u(\vec{r},\omega_t)+k(\omega_t)^2 u(\vec{r},\omega_t)=-\frac{q(\vec{r},\omega_t)}{D}, \tag{1}$$

$$k(\omega_t)^2=\frac{-\nu\mu_a-i\omega_t}{D}, \tag{2}$$

$$D=\frac{\nu}{3\mu_s'}, \tag{3}$$

$$u_0(\vec{r})=\frac{i}{4D}H_0^{(1)}(k(\omega_t)|\vec{r}_{yz}-\vec{r}_{yz}^{\,0}|). \tag{4}$$

If the first Born approximation for an absorption heterogeneity is applied to Eq. (1) then the resulting perturbation in the photon density is given by:

$$(\nabla^2+k(\omega_t)^2)u_s(\vec{r},\omega_t)=\frac{\nu\delta\mu_a(\vec{r})}{D}u(\vec{r},\omega_t) \tag{5}$$

where $\delta\mu_a(\vec{r})$ is the absorption perturbation, $u_0(\vec{r},\omega_t)$ is the photon density in the absence of any perturbation, in this case given by (4), and $u_s(\vec{r},\omega_t)$ is the perturbation in the photon density, being the total photon density $u(\vec{r},\omega_t)=u_0(\vec{r},\omega_t)+u_s(\vec{r},\omega_t)$. Assuming that $u_0(\vec{r}_{yz},\omega_t) >> u_s(\vec{r}_{yz},\omega_t)$, the solution to Eq. (5) has an integral form (6) that can be written in terms of the equation's Green's function. Some authors use this triple integral to formulate the equation system that will be inverted to reconstruct the objects that produced the perturbations in the measured photon density. The problem's complexity however increases linearly with the number of voxels.

$$u_s(\vec{r},\omega_t)=-\int\int\int g(\vec{r}|\vec{r}\,',\omega_t)\frac{\nu\delta\mu_a(\vec{r}\,')}{D}u_0(\vec{r}\,',\omega_t)d\vec{r}\,', \tag{6}$$

In order to reduce the complexity of the problem, we apply Fourier in the x domain to Eq. (5), yielding:

$$(\nabla_{yz}^2+(i\gamma_x(\omega_t))^2)u_s(\vec{r}_{yz},q_x,\omega_t)=\frac{\nu\delta\mu_a(q_x,\vec{r}_{yz})}{D}u(\vec{r}_{yz},\omega_t), \tag{7}$$

$$\gamma_x(\omega_t)^2=q_x^2-k(\omega_t)^2 \tag{8}$$

where q_x is the spatial frequency in the x direction. The Green's function of (7) is (9), and its solution can therefore be expressed in its terms as shown in Eq. (10)

$$g(\vec{r}|\vec{r}\,')=\frac{i}{4}H_0^{(1)}(i\gamma_x(\omega_t)|\vec{r}_{yz}-\vec{r}\,'_{yz}|), \tag{9}$$

$$u_s(\vec{r}_{yz},q_x,\omega_t)=-\int\int\frac{\nu\delta\mu_a(q_x,\vec{r}\,'_{yz})}{D}u_0(\vec{r}\,'_{yz},\omega_t)\frac{i}{4}H_0^{(1)}(i\gamma_x(\omega_t)|\vec{r}_{yz}-\vec{r}\,'_{yz}|)d\vec{r}\,'_{yz}. \tag{10}$$

Given the fact that it is possible to measure u_s in the reception plane, an equation system can be formulated for each spatial frequency q_x, where u_s is defined for each different combination of y position and time modulation frequency ω_t, reducing the complexity of each equation system from 3 dimensions to only 2. Once $\delta\mu_a(q_x,\vec{r}_{yz})$ is resolved for each q_x, then $\delta\mu_a(\vec{r})$ can be simply calculated with an inverse Fourier transform.

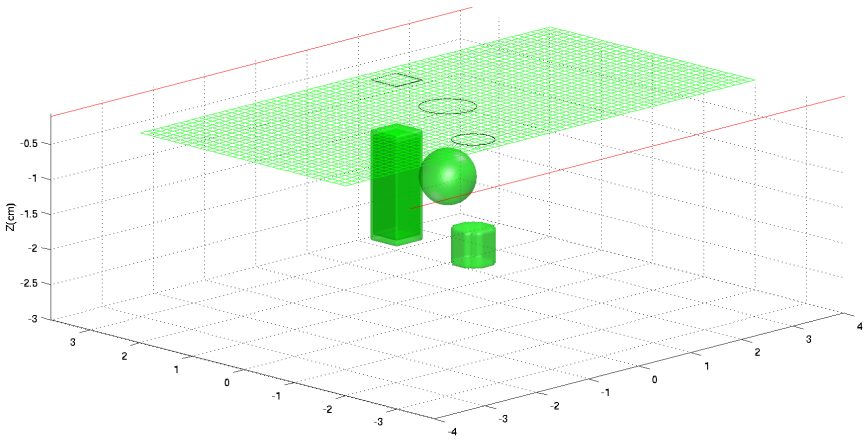

Figure 2. Setup used in the simulations. The entire volume represents the intralipid phantom with three different embedded objects. The XY plane at Z=0cm is where the light is projected and measured. The red lines represent the laser line sources and the green grid the field of view of the camera, the black rectangles are the projections of the heterogeneities on the XY plane.

4. RESULTS

A new reconstruction algorithm has been implemented based on the theory described above. Its main advantage resides in the fact that it works with all the sources superimposed and uses the information in the time frequency domain to invert the integral Eq. (6). Hence, it is not necessary to perform a measurement for each source, and thus much faster the acquisitions can be achieved. The algorithm also exploits the source geometry to reduce the complexity of the system of equations to be inverted by applying Fourier in the x spatial domain. The algorithm we implemented is a derivation of the previously described formula (10) that takes into account the fact that we are working in a semi-infinite medium and that we measure the photon flux on the surface of the medium, not directly the photon density.

We performed simulations with our model to evaluate the performance of the reconstruction algorithm in the absence of noise. As described in literature,[9] the problem is ill posed by nature, due to the absorbing nature of the medium and the limited measurement points on the surface. For this reason, regularization is a key factor when resolving the system of equations.We performed several simulations with different inversion algorithms. The setup that we simulated is shown in Figure 2. The reconstructions for the different methods are shown in Figure 3. The best results were obtained using the sub-space preconditioned least square root (SP-LSQR) algorithm[10] with a cosines basis and a customized linear operator that optimized the result. SP-LSQR is an iterative algorithm that uses Tikhonov regularization together with the classical iterative LSQR algorithm. In order to find the solution to the equation system it tries to minimize the following formula:

$$||Ax - b||^2 + \lambda||Lx||^2. \tag{11}$$

where A is the matrix defining the equation system, b are the constant terms, x the unknowns, L is a linear operator that defines a suitable smoothing norm for the problem and λ is the regularization parameter that controls the weight between the residual and smoothing norms.[10]

Figure 4a shows an experiment performed with a homogeneous phantom with $\mu_a = 0.07cm^{-1}$ and $\mu_s' = 5cm^{-1}$, with two embedded 5mm diameter cylinders with $\mu_a = 0.25cm^{-1}$ and $\mu_s' = 5cm^{-1}$. The cylinders are 1cm deep in the phantom and they are separated 5mm from each other. Figure 4b shows the reconstruction obtained from the experimental data. We can clearly distinguish two objects embedded in the phantom. Only one section of the cylinders is detected accurately, this is due to the fact that there is not enough light illuminating the other half of the cylinders. This will be overcome by adding a second source at the other side of the detector in the future. Despite, the current limitations, our prototype demonstrates a target detection consistent with a spatial uncertainty of less than 5mm, thus showing the suitability of the approach to the target applications.

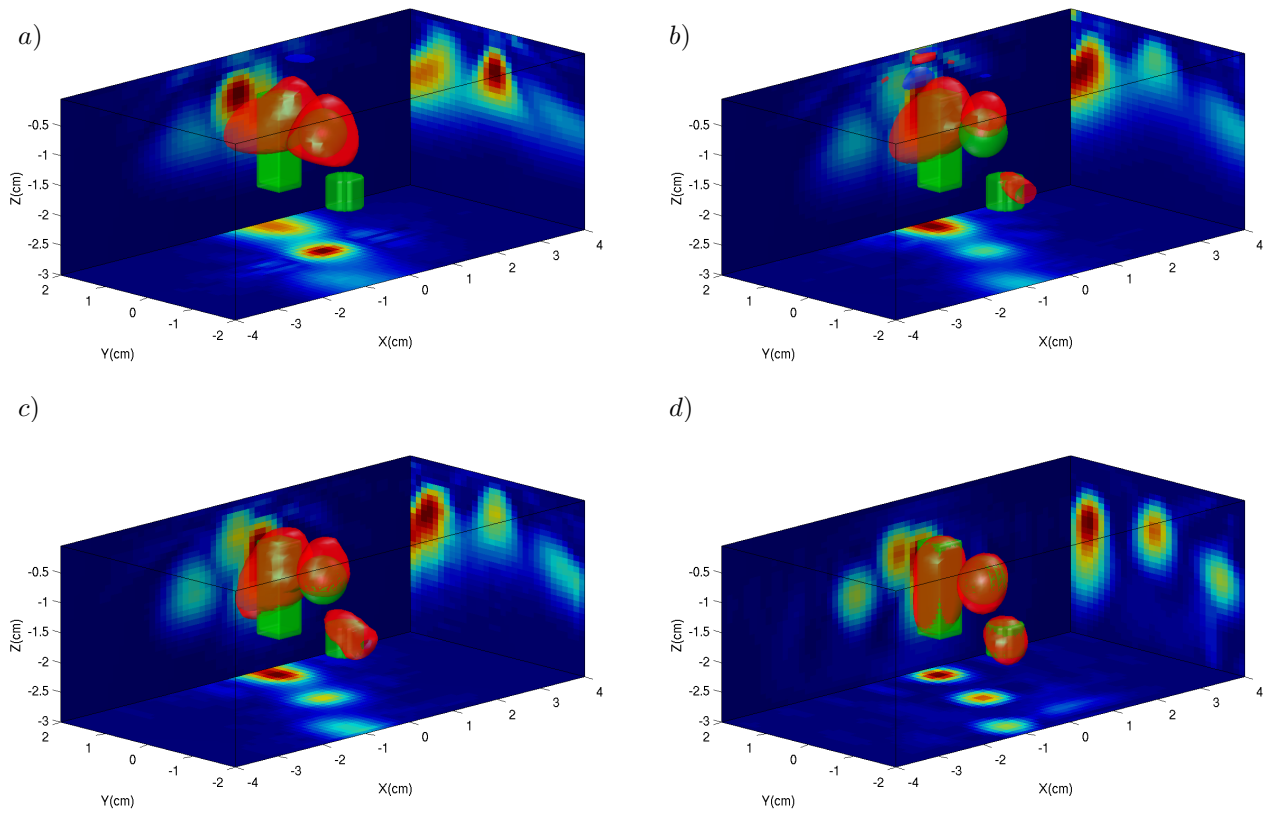

Figure 3. Reconstructions from simulated data performed with different methods: a) Algebraic Reconstruction Technique (ART), b) Conjugate Gradient (CG), c) SPLSQR with identity operator as regularization term, d) SPLSQR with customized linear operator as regularization term.

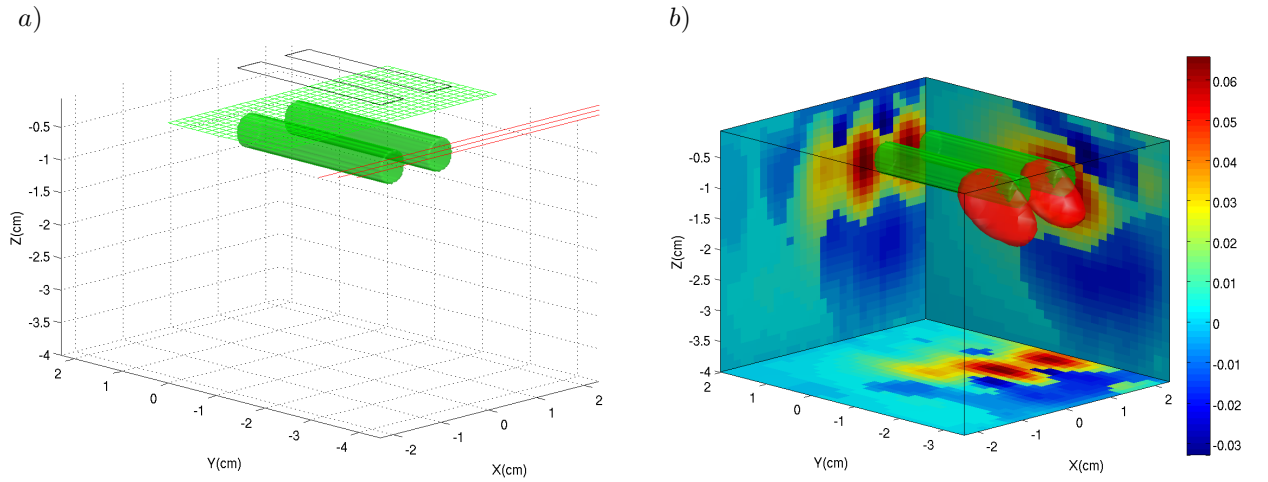

Figure 4. a) Setup used in measurements to evaluate the system resolution and reconstruction accuracy. The volume represents the intralipid phantom with two 5mm diameter cylinders separated 5mm from each other. b) Reconstruction from the experimental measurement. The green volumes represent the original objects, while the red ones are the reconstructed ones.

5. CONCLUSIONS

In this contribution we demonstrated how SPAD imagers make time-resolved high spatial resolution measurements for 3D NIRI possible, filling the gap between low resolution time-resolved measurements and high resolution CW measurements.

The new algorithm reduces the complexity of the reconstructions making it possible to parallelize the computations and enabling higher resolutions.

It has been demonstrated that a resolution of at least 5mm can be obtained with the presented setup. We are planning to upgrade the setup so it can be used with multiple light sources and thus be able to reconstruct bigger areas. We expect as well that with more light sources the resolution of the system will improve significantly.

ACKNOWLEDGMENTS

We would like to acknowledge the work of Cristiano Niclass who designed the SPAD sensor used in this research.

REFERENCES

[1] Markel, V. A. and Schotland, J. C., "Inverse problem in optical diffusion tomography. I. Fourier-Laplace inversion formulas," *J. Opt. Soc. Am. A* **18**, 1336–1347 (Jun 2001).

[2] Abookasis, D., Lay, C. C., Mathews, M. S., Linskey, M. E., Frostig, R. D., and Tromberg, B. J., "Imaging cortical absorption, scattering, and hemodynamic response during ischemic stroke using spatially modulated near-infrared illumination," *J Biomed Opt* **14**, 024033 (2009).

[3] Konecky, S. D., Mazhar, A., Cuccia, D., Durkin, A. J., Schotland, J. C., and Tromberg, B. J., "Quantitative optical tomography of sub-surface heterogeneities using spatially modulated structured light," *Opt. Express* **17**, 14780–14790 (Aug 2009).

[4] Cai, W., Gayen, S. K., Xu, M., Zevallos, M., Alrubaiee, M., Lax, M., and Alfano, R. R., "Optical tomographic image reconstruction from ultrafast time-sliced transmission measurements," *Appl. Opt.* **38**, 4237–4246 (Jul 1999).

[5] Ntziachristos, V., Ripoll, J., Wang, L. V., and Weissleder, R., "Looking and listening to light: the evolution of whole-body photonic imaging," *Nat. Biotechnol.* **23**, 313–320 (Mar 2005).

[6] Niclass, C., Favi, C., Kluter, T., Gersbach, M., and Charbon, E., "A 128 128 single-photon image sensor with column-level 10-bit time-to-digital converter array," *Solid-State Circuits, IEEE Journal of* **43**(12), 2977–2989 (2008).

[7] Pifferi, A., Torricelli, A., Spinelli, L., Contini, D., Cubeddu, R., Martelli, F., Zaccanti, G., Tosi, A., Dalla Mora, A., Zappa, F., and Cova, S., "Time-resolved diffuse reflectance using small source-detector separation and fast single-photon gating," *Phys. Rev. Lett.* **100**, 138101 (Mar 2008).

[8] Torricelli, A., Pifferi, A., Spinelli, L., Cubeddu, R., Martelli, F., Del Bianco, S., and Zaccanti, G., "Time-resolved reflectance at null source-detector separation: improving contrast and resolution in diffuse optical imaging," *Phys. Rev. Lett.* **95**, 078101 (Aug 2005).

[9] O'Leary, M. A., *Imaging with diffuse photon density waves*, PhD thesis, University of Pennsylvania (1996).

[10] Jacobsen, M., Hansen, P., and Saunders, M., "Subspace preconditioned lsqr for discrete ill-posed problems," *BIT Numerical Mathematics* **43**, 975–989 (2003). 10.1023/B:BITN.0000014547.88978.05.